SF2A 2016
C. Reylé, J. Richard, L. Cambrésy, M. Deleuil, E. Pécontal, L. Tresse and I. Vauglin (eds)

21CM BISPECTRUM AS METHOD TO MEASURE COSMIC DAWN AND EOR

H. Shimabukuro[1]

Abstract. Cosmological 21cm signal is a promising tool to investigate the state of the Inter Galactic Medium (IGM) during cosmic dawn (CD) and Epoch of Reionization (EoR). Ongoing telescopes such as MWA,LOFAR,PAPER and future telescopes like SKA are expected to detect cosmological 21cm signal. Statistical analysis of the 21cm signal is very important to extract information of the IGM which is related to nature of galaxies and first generation stars. We expect that cosmological 21cm signal follows non-gaussian distribution because various astrophysical processes deviate the distribution from gaussian. In order to evaluate the non-gaussian features, we introduce the bispectrum of the 21cm signal and discuss the property of the 21cm bispectrum such as redshift dependence and configuration dependence. We found that the we can see correlation between large scales and small scales via the 21cm bispectrum and also found that the 21cm bispectrum can give the information of matter fluctuation, neural fraction fluctuation and spin temperature fluctuation by means of its configure dependence.

Keywords: cosmology: dark ages, reionization, first stars

1 Introduction

The redshifted 21cm line from neutral hydrogen due to the hyperfine transition is suitable for studying thermal and ionized states of Inter Galactic Medium (IGM) as well as the first objects in the dark age, cosmic dawn (CD) and Epoch of Reionization (EoR) (Furlanetto et al 2006; Pritchard & Loeb 2012). One of the statistical methods to subtract the information about the physical state of IGM at those epochs from 21cm line is the power spectrum analysis of brightness temperature (Furlanetto et al 2006; Pritchard & Furlanetto 2007; Santos et al. 2008; Baek et al. 2010; Mesinger et al. 2013; Pober et al. 2014).

In our previous work Shimabukuro et al. (2015), we gave an interpretation to the time evolution of the 21cm power spectrum and we find that the size of skewness is sensitive to the epoch when X-ray heating becomes effective. Herein we extend this previous work by considering the the bispectrum to investigate the dependence of the skewness on scales because skewness is an integral of the bispectrum with respect to the wave number. In a different work Yoshiura et al. (2015) we have already estimated errors from the thermal noise of detectors in estimating the bispectrum and we found that the 21cm bispectrum would be detectable at large scales at $k \leq 0.1\mathrm{Mpc}^{-1}$ even by the current detectors, such as, the MWA and PAPER. In our study, we focus on non-Gaussianity in 21cm fluctuations induced by astrophysical effects not by cosmological origin. For other probes of non-Gaussianity such as Minkowski functionals, see Gleser et al. (2006); Yoshiura et al. (2016).

2 Formulation and set up

A fundamental quantity of 21cm line is the brightness temperature, which is described as the spin temperature offsetting from CMB temperature, given by (see, e.g. Furlanetto et al 2006)

$$\begin{aligned}\delta T_b(\nu) &= \frac{T_\mathrm{S}-T_\gamma}{1+z}(1-e^{-\tau_{\nu_0}}) \\ &\sim 27 x_\mathrm{H}(1+\delta_m)\left(\frac{H}{dv_r/dr+H}\right)\left(1-\frac{T_\gamma}{T_\mathrm{S}}\right) \\ &\times \left(\frac{1+z}{10}\frac{0.15}{\Omega_m h^2}\right)^{1/2}\left(\frac{\Omega_b h^2}{0.023}\right)[\mathrm{mK}]. \end{aligned} \quad (2.1)$$

[1] Observatoire de Paris, 61 Avenue de l'Observatoire, 75014 Paris, France

Here, $T_{\rm S}$ and T_γ respectively represent gas spin temperature and CMB temperature, τ_{ν_0} is the optical depth at the 21cm rest frame frequency $\nu_0 = 1420.4$ MHz, $x_{\rm H}$ is neutral fraction of the hydrogen gas, $\delta_m(\mathbf{x}, z) \equiv \rho/\bar{\rho} - 1$ is the evolved matter overdensity, $H(z)$ is the Hubble parameter and dv_r/dr is the comoving gradient of the gas velocity along the ling of sight. All quantities are evaluated at redshift $z = \nu_0/\nu - 1$.

Let us focus on the spatial distribution of the brightness temperature. The spatial fluctuation of the brightness temperature can be defined as

$$\delta_{21}(\mathbf{x}) \equiv \delta T_b(\mathbf{x}) - \langle \delta T_b \rangle \tag{2.2}$$

where $\langle \delta T_b \rangle$ is the mean brightness temperature obtained from brightness temperature map and $\langle ... \rangle$ expresses the ensemble average. If the statistics of the brightness temperature fluctuations is pure Gaussian, the statistical information of the brightness temperature should be completely characterized by the power spectrum. However, in the era of CD and EoR, it is expected that the spin temperature and the neutral fraction should be spatially inhomogeneous and the statistics of the spatial fluctuations of those quantities would be highly non-Gaussian due to the various astrophysical effects. Here, in order to see the non-Gaussian feature of the brightness temperature fluctuations δ_{21}, we focus on the bispectrum of δ_{21} which is given by

$$\langle \delta_{21}(\mathbf{k_1})\delta_{21}(\mathbf{k_2})\delta_{21}(\mathbf{k_3}) \rangle = (2\pi)^3 \delta(\mathbf{k_1} + \mathbf{k_2} + \mathbf{k_3}) B(\mathbf{k_1}, \mathbf{k_2}, \mathbf{k_3}). \tag{2.3}$$

In order to characterize the shape of the bispectrum in k-space, we use an isosceles ansatz which is defined as $k_1 = k_2 = k = \alpha k_3$ ($\alpha \geq 1/2$). For examples, in case with $\alpha \gg 1$ the shape of the bispectrum is often called as "*squeezed type*" or "*local type*", in case with $\alpha = 1$ it is called as " *equilateral type*", and in case with $\alpha = 1/2$ it is called as "*folded type*".

3 Result

In this section, we summarize our result for the 21cm bispectrum.

3.1 Redshift evolution of 21cm bispectrum

Next, we consider redshift evolution of 21cm bispectrum. We show ionized evolution and the bispectra as functions of redshift for several α in Fig. 1: the equilateral shape ($\alpha = 1$), the folded shape ($\alpha = 1/2$) and the squeezed shape ($\alpha = 10$) with $k = 1.0$ Mpc^{-1}. For the equilateral and folded cases, we can see two peaks located at around $z = 20$ and 12. These peaks can also be seen in the power spectrum of the brightness temperature fluctuations, $P_{21}(k)$, with $k \simeq 1.0$ Mpc^{-1} (see, e.g., our previous paper Shimabukuro et al. 2015). On the other hand, in case with the squeezed shape, three peaks appear at around $z = 23$, 17, and 12. This feature is similar to that of the power spectrum with $k \simeq 0.1$ Mpc^{-1} (Shimabukuro et al. 2015). For the squeezed type, we take the parameter α to be 10 and this means $k_3 = 0.1$ Mpc^{-1}. Hence, the squeezed-type 21cm bispectrum is expected to be described in terms of not only the power spectrum with larger two wave number (k_1 and k_2 in our case) but also that with smaller one wave number (k_3 in our case) and also it would have the information about the correlation between the long and short wavelength modes in Fourier space or local non-linearity in real space. The dip at $z \sim 20$ for the $\alpha = 10$ case results in mode coupling between long and short wavelengths. Therefore, we can conclude that the squeezed type bispectrum has information both on large scale and small scale.

3.2 Decomposition of 21cm bispectrum

As we saw in Eq. (2.1), the fluctuations in the brightness temperature are contributed not only from the matte density field, but also from the fluctuations of the spin temperature and neutral fraction, aside from the gradient of peculiar velocity which we neglect here. In this section, we decompose the bispectrum into the contributions from these components.

We can rewrite Eq. (2.1) as,

$$\delta T_b(\mathbf{x}) = \overline{\delta T}_b (1 + \delta_{x_{\rm H}}(\mathbf{x}))(1 + \delta_m(\mathbf{x}))(1 + \delta_\eta(\mathbf{x})), \tag{3.1}$$

where $\overline{\delta T_b}$ is the average brightness temperature.

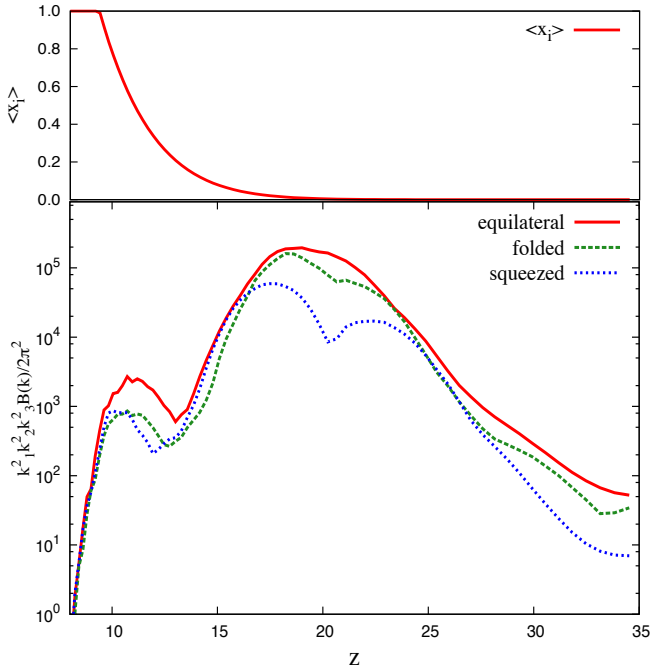

Fig. 1. (*Top*) ionization history in our model. (*Bottom*) Comparison of bispectra of typical triangle configurations. We fix $k = 1.0$ Mpc^{-1} and take $\alpha = 1$ (equilateral: red solid line), $\alpha = 1/2$ (folded: green dashed line) and $\alpha = 10$ (squeezed: blue dotted line) for the isosceles ansatz.

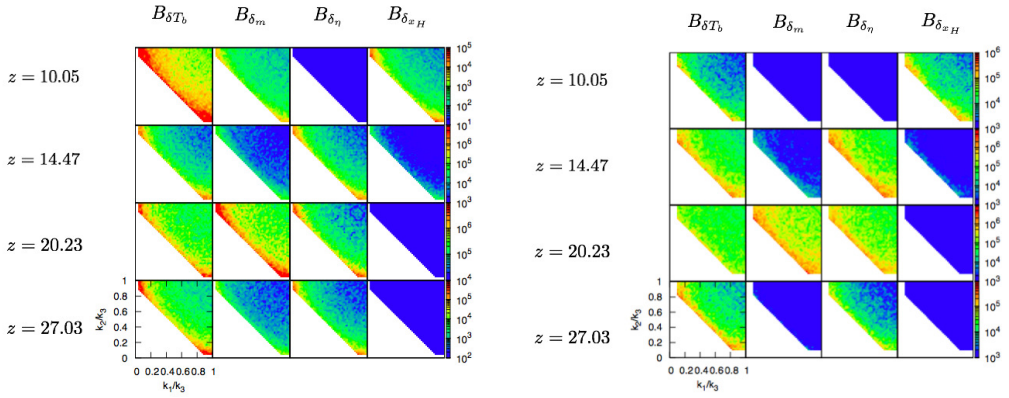

Fig. 2. (*Left*) Contours of the total bispectrum and its components in k_1/k_3-k_2/k_3 plane with $k_3 = 1.0$ Mpc^{-1}. (*Right*) Contours of the total bispectrum and its components in k_1/k_3-k_2/k_3 plane with $k_3 = 0.4$ Mpc^{-1}.

Here we characterize the contribution of the spin temperature T_s by a new variable $\eta = 1 - T_\gamma/T_{\rm S}$ (Shimabukuro et al. 2015). Using Eq. (3.1), we can decompose the brightness temperature bispectrum into auto- and cross-correlation of $\delta_m, \delta_{x_{\rm H}}$ and δ_η:

$$\begin{aligned} B_{\delta T_b} &= (\overline{\delta T}_b)^3[B_{\delta_m\delta_m\delta_m} + B_{\delta_{x_{\rm H}}\delta_{x_{\rm H}}\delta_{x_{\rm H}}} + B_{\delta_\eta\delta_\eta\delta_\eta} \\ &\quad +(\text{cross correlation terms}) \\ &\quad +(\text{higher order terms})]. \end{aligned} \tag{3.2}$$

We focus on the shape dependence of the total bispectrum and its components. Fixing $k_3 = 1.0$ Mpc^{-1}, we

plot contours of the bispectra in (k_1/k_3)-(k_2/k_3) plain in left of Fig. 2. Note that we do not use the normalised bispectrum, $k_1^2k_2^2k_3^2B(k_1,k_2,k_3)$, but the unnormalized bispectrum, $B(k_1,k_2,k_3)$, here. We can see in what configuration of triangle the bispectra are strong. Here it should be noted that the triangle condition is not satisfied in the blank region.

At $z = 10.05$ when EoR has proceeded to some extent($x_i = 0.77$), the total bispectrum is strong at folded and squeezed types. The contribution from neutral hydrogen fraction fluctuations is dominant at these configurations, while matter fluctuation is dominant at equilateral type. At $z = 14.47$, the dominant contribution comes from the spin temperature fluctuations and it is largest at squeezed type. The situation is similar at $z = 27.03$. At $z = 20.23$, both squeezed and folded type of the total bispectrum are strong. The contributions from matter and spin temperature fluctuations are comparable at these configurations, while the former is dominant at equilateral type.

We also show the contour for $k_3 = 0.4$ Mpc^{-1} in the right of Fig.2. Compared with the case of $k_3 = 1.0$ Mpc^{-1}, contributions from both matter and spin temperature fluctuations are significant at $z = 20.23$. On the other hand, we find that the contribution from fluctuations of neutral hydrogen fraction at $z = 10.05$ is clear compared with the case of $k_3 = 1.0$ Mpc^{-1}. This helps us to subtract the information on neutral hydrogen and it is better to see larger scales if we would like to know the information on neutral hydrogen fluctuations.

4 Conclusions

In this proceeding, we introduced the 21cm bispectrum as method to measure non-Gaussianity of brightness temperature field generated by astrophysical processes.

First, we have shown the redshift evolution of the 21cm bispectrum with fixed k for three types of the shape in k-space. We found that the redshift evolution of the 21cm bispectrum for the equilateral and folded shapes basically traces that of the 21cm power spectrum, but in case with the squeezed shape, we could see a different behavior and it can be understood by considering the coupling between the large- and small-scale modes.

Next, we studied the 21cm bispectrum by decomposing it into the contributions from the matter density field, the fluctuations in the spin temperature and the neutral fraction. From the redshift evolution, we found the dominant component at each redshift and scale. We also show the shape dependence of each component and compared it with that of total 21cm bispectrum. The shape dependence of each component looks similar to each other, but a slight difference also exists. Hence, by future precise observation it is expected that we would obtain the information about the non-Gaussian feature of these components separately.

5 Acknowledements

This work is supported by Grant-in-Aid from the Ministry of Education, Culture, Sports, Science and Technology (MEXT) of Japan, No. 25-3015 and a grant from the French ANR funded project ORAGE (ANR-14- CE33-0016)

References

S. Baek, B. Semelin, P. Di Matteo, Y. Revaz and F. Combes, arXiv:1003.0834 [astro-ph.CO].

X. H. Fan, C. L. Carilli and B. G. Keating, Ann. Rev. Astron. Astrophys. **44** (2006) 415 [astro-ph/0602375].

S. Furlanetto, S. P. Oh and F. Briggs, Phys. Rept. **433** (2006) 181 [astro-ph/0608032]

L. Gleser, A. Nusser, B. Ciardi, & V. Desjacques 2006, MNRAS, 370, 1329

A. Mesinger, S. Furlanetto, R. Cen,2011, MNRAS, 411, 955

A. Mesinger, A. Ewall-Wice and J. Hewitt, arXiv:1310.0465 [astro-ph.CO]

J. C. Pober, A. Liu, A, J. S. Dillon, et al. 2014, ApJ, 782, 66

J. R. Pritchard and S. R. Furlanetto, Mon. Not. Roy. Astron. Soc. **376** (2007) 1680 [astro-ph/0607234]

Pritchard, J. R., & Loeb, A. 2012, Reports on Progress in Physics, 75, 086901

M. G. Santos, A. Amblard, J. Pritchard et al. 2008, ApJ, 689, 1

H. Shimabukuro, S. Yoshiura, K. Takahashi, S. Yokoyama. & Ichiki, K. 2015, Mon. Not. Roy. Astron. Soc. , 451, 4986

S. Yoshiura, H. Shimabukuro, K. Takahashi, et al. 2015, Mon. Not. Roy. Astron. Soc. 451, 4785

Yoshiura, S., Shimabukuro, H., Takahashi, K., & Matsubara, T. 2016, arXiv:1602.02351